Contribution of Hexagonal-like Structure to the Nonlinear Optics in SiC Nanocrystallites

K.J.Plucinski*, I.V.Kityk**, and A. Kassiba***

*Military University of Technology, 00-908 Warsaw, Poland, kpluc@wel.wat.waw.pl
**Institute of Physics, University WSP, Ul.Gombrowicza 1/144, PL-42201 Cz_stochowa, Poland
***Laboratoire de Physique de l'Etat Condense UPRES-A6087, Universite du Maine, Avenue Olivier Messiaen 72085 Le Mans Cedex 9, France

ABSTRACT

The influence of the degree of hexagonality on the photoinduced second harmonic generation (PISHG) in SiC large-sized nanocrystallites, with sizes ranging from 10 – 30 nm and incorporated into an oligoetheracrylate photopolymer matrix was investigated. The PISHG measurements were carried out using pulsed YAG:Nd laser (λ=1.06 μm, duration time τ= 15 - 50 ps, laser power about 30 MW) as probing beam and a Q-switched nitrogen pulse laser (P=10 MW, λ=0.377 μm, τ=5-15 ps) as photoinducing beam. Molecular dynamics simulations and band structure calculations enabled us to establish the relation between nanocrystallite size, band structure and degree of hexagonality (partial presence of the hexagonal structural component). Quantum chemical simulations of the PISHG versus temperature, pump-probe time delay and degree of hexagonality were carried out.

Keywords: SiC nanocrystallites, photoinduced second harmonic generation measurements, molecular dynamic simulation.

1 INTRODUCTION

Many studies have been made of changes in band structure due to confinement-induced quantization of continuous band states [1–9]. Main experimental approaches when investigating nanocrystallites have traditionally focused on different optical methods, particularly those based on fluorescence [10], Raman scattering[11-12], photon echo[13-14], electroluminescence and absorption [15-16]. These works have shown that a decrease in nanocrystallite size leads to changes in electronic structure and the relevant optical spectra [17,18]. They have established that this is due to the size scaling of electron transitions and electron-phonon interactions [2-4], including anharmonic electron-phonon interactions [9].

All the known theoretical methods may be divided into two main groups. The first are based on a long-range ordering solid state approach [19]. Most of the calculations within the framework of this bulk-like approach are made using semi-empirical band energy calculations. In the second group, the nanocrystallites are constructed as a large molecule, and a molecular cluster approach is applied [20]. Neither of these broad approaches make it possible to correctly take into account the relation between long-range order and local disordering, particularly near the interfaces.

Quasi-Brillouin-zone, self-energy corrections, exciton Coulomb energies, and optical gaps in quantum dots have also been calculated [21] from first principles using a real space pseudopotential method. The calculations were carried out on spherical clusters with up to 800 Si and H atoms. It was demonstrated that self-energy corrections improved the results of calculations for all nanocrystallites, though most markedly for quantum dots. This improvement was most significant when size and wave function parameters were varied at the same time. Quantum confinement and reduced electron screening were also found to result in appreciable exciton Coulomb energies.

Of particular interest are so-called large-sized nanocrystallites (larger than 10 nm)[7]. These are, on the one hand, nanocrystallites which are, due to their small size, affected by disturbances at interface regions. On the other hand, they have properties typical for bulk-like crystals. These latter properties make it possible to apply the **k**-dispersion approach (Bloch theorem). Large-sized nanocrystallites provide promising potential for the creation of materials with enhanced nonlinear optical response susceptibilities, because the smaller the nanocrystallite, the larger the contribution originating from interface electrostatic potential gradients. These gradients determine enhanced dipole moments on the surface and are important for inducing nonlinear optical effects at the interface due to high gradients between the ordered and disordered structural phases.

For the purposes of our investigation, we chose SiC nanocrystallites with relatively large sizes (10 –30 nm). The main reasons for this choice were as follows:

- the technology of SiC nanocrystallites with suitable sizes is better developed than that for other semiconducting materials [22];
- the relatively large sizes (10 – 30 nm) make it possible to use one-electron band energy calculation methods in the **k**-space [21];
- the high mechanical and chemical stability of

nanocrystallites;

- the possibility of effective variation of energy gaps by varying the ratio between hexagonal-like and cubic phase;
- expected high nonlinear optical response caused by a high degree of hexagonality.

For our theoretical simulation, we extended an approach developed for partially disordered materials, such as glasses [23-24], organic molecules [25], disordered crystals [26].

The main steps of our approach are as follows:

- band energy calculations within the framework of a norm-conserving pseudopotential local density approximation (LDA) with different ratios of cubic and hexagonal-like phases;
- molecular dynamics geometry optimization of the interface (amorphous-like-nanocrystallite) region;
- simulation of electronic and optical properties of the interface structural components;
- evaluation of the relation between interface geometry, nanocrystallite sizes and the photoinduced nonlinear optical response versus temperature and pump-probe delaying time. Electron-phonon interactions were also taken into account.

2 RESULTS AND DISCUSSIONS

The measured dependencies of photoinduced SHG as a function of pump power I_0 are presented in Fig. 1. Photoinduced fluorescence measurements show that the main fluorescence maxima lie at 450-496 nm spectral range and do not overlap with the green light PISHG signal observed. The coherence length was found to be about 1.2 μm which is comparable with the sizes of the nanocrystallites investigated. The output PISHG signal was equal to about $10^{-4} – 10^{-5}$ of the incident probe YAG-Nd laser intensity. In order to calculate the PISHG values, we also measured transparency and reflection spectra within the 500 – 1100 nm spectral range. The corresponding corrections were introduced into the expression for appropriate calculations of the χ_{xxxx} tensor. Here, direction x is chosen parallel to the photoinducing UV-beam polarization. The scattered background was measured independently with the corresponding corrections taken into account. The Kerr effect was measured using the traditional Senarmont method, with precision of birefringence determination of about 10^{-5}. All the measurements were made during UV- illumination. For each I_0 value, we obtained PISHG values for more than 120 points. The (^{2} parameter of Student statistics was better than 4.5 %. The PISHG was determined with accuracy up to 10^{-2} pm/V.

It is important to note that the oligoetheracrylate photopolymer matrices make it possible to continuously vary the refractive indices in order to minimize light scattering losses. At the same time, these matrices have relatively low nonlinear optical susceptibilities and, at the border between the nanocrystallites and photopolymer

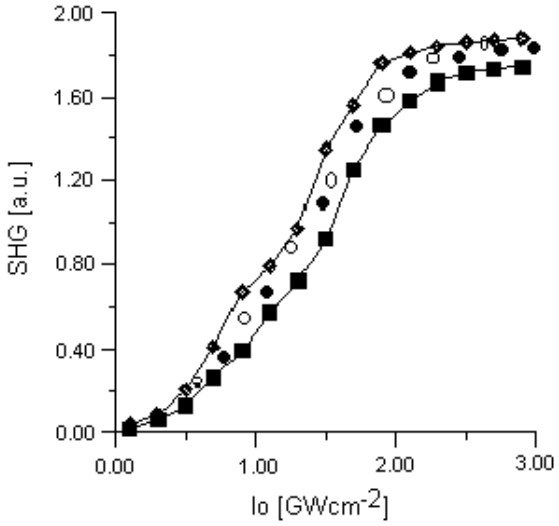

Fig. 1. Experimental dependence of the PISHG versus the UV-photoinducing beam power for different degrees of hexagonality: ♦- 0.75; h-0.66; o -0.34; g - 0.21.

background, the corresponding susceptibilities are at least one order less than at the border between the nanocrystallites and amorphous-like SiC background.

With increasing I_0, the PISHG maximum output signal increases and achieves its maximum at Q-switched nitrogen-laser photoinducing power values lying within the range 2.1 – 2.2 GW/cm^2 per pulse (this corresponding to electric field of between $10^7 – 10^8$ V/m). This field causes significant redistribution of the birefringence due both to the optical Kerr effect, as well as to the charge carrier redistribution.

The experimentally measured PISHG values were in good agreement with those theoretically predicted. The maximum output PISHG was observed for collinear polarization of probe and pump light beams and incident angles lying within 5 – 7^o with respect to the surface. We found also that the lowest scattered background was obtained for a spot where the probe laser beam was about 52 – 64 μm. All the photoinduced changes were reversible, with precision up to 0.036 % (from measurements of photoabsorption and reflection). The maximum intensity of the output PISHG was achieved for a time delay of about 20 ps and at low temperatures (below 15 K). The calculated PISHG is presented versus the degree of hexagonality (H), and one can clearly see that an increase in the (H) up to 0.75 enhances the output PISHG signal by at least 16 %.

The off-diagonal χ_{xxy}, χ_{yyx},χ_{xyx} tensor components were at least half an order weaker than diagonal components. The PISHG tensor components are very sensitive to photoinduced birefringence. During evaluations of the corresponding tensor components, we therefore renormalized appropriate values under phase synchronism

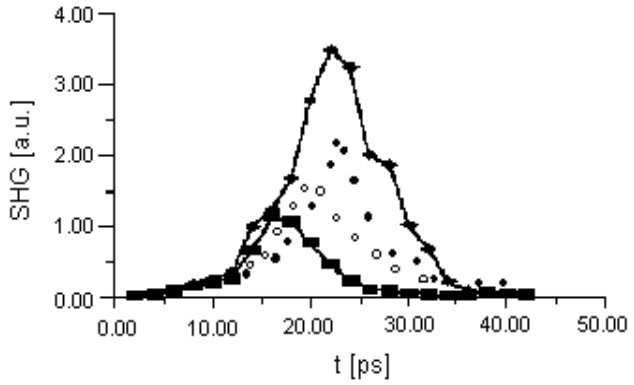

Fig. 2. Experimental time delay dependences of the PISHG for different degrees of hexagonality: ♦ - 0.66; h - 0.42; o - 0.30; g - 0.22.

conditions which are largely dependent on the photoinduced birefringence.

By continuously varying the time delay between the pump and probe beams, we observed a PISHG maximum for the pump-probe time delays of about 18 – 22 ps (see Fig. 2). The pump-probe time positions of the PISHG maxima are seen to be dependent on the hexagonality (H). In agreement with theoretical predictions, one can see a shift of the SHG maxima towards the higher time delays (t) with an increase in (H). The experimental PISHG dependencies observed are very similar to those theoretically calculated. The differences which do occur are independent of (H). The main discrepancies are found in the values of the PISHG maxima. This is probably due to the effect of specimen non-homogeneity, disturbances to phase-matching conditions, as well as to light scattering. The PISHG dependencies measured also show a weak time-dependent asymmetry. For time delays higher than 36 ps, the output PISHG signal becomes very low (comparable with the noise background). The PISHG values change within the range 0.68 – 0.98 pm/V.

We carried out PISHG measurements versus temperature (within the temperature range 4.2 – 50 K) at different (H) (see Fig. 3). All the measurements were conducted for a pump-probe time delay of about 20 ps. The maximum PISHG signal was achieved within the temperature range 4.2 – 18 K and the PISHG value is increased up to 0.90 pm/V for the $H \approx 0.75$. This fact indicates on an agreement between the theoretically calculated and experimentally evaluated (see Fig. 3) PISHG features.

It is necessary to add that at temperatures higher than 70 K, the PISHG signal is comparable to the light scattering background (due to temperature reorientation). One can also see several temperature-dependent steps in the PISHG behavior observed. The photoinduced PISHG signal relaxation time never exceeds 1.7 ps, and decreases to 0.83 ps for temperatures higher than 42 K.

Picosecond relaxation times indicate on a substantial contribution of electron-phonon interactions to the

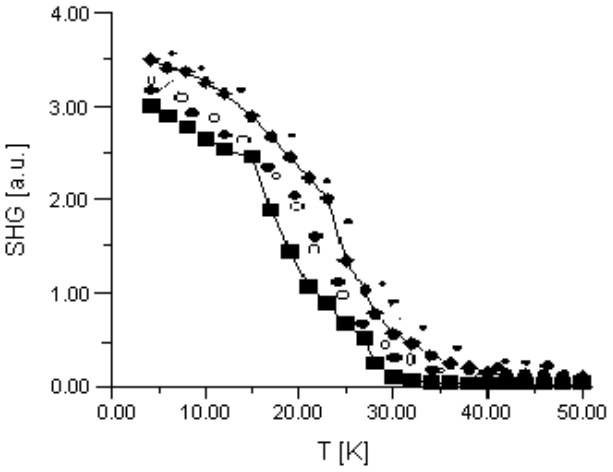

Fig. 3. Experimental temperature dependences of the PISHG for different degrees of hexagonality: • - 0.75; ♦- 0.66; n - 0.42; o - 0.34; g - 0.21. All the data has been renormalised for the same photoinduced conditions.

observed photoinduced SHG changes.

The photoexcited phonons contribute additionally to the temperature-dependent PISHG due to a high degree of anharmonic electron-phonon interaction.

The performed work shows essential role of the surfaces and hexagonality of the nanocrystallites and surrounding amorphous-like background in appearance of the local non-centrosymmetry. The latter causes hyperpolarizabilities essentially higher than for the bulk-like crystals as well as for the polymer-like molecule.

3 CONCLUSIONS

For the first time an essential photoinduced PISHG in the SiC large-sized nanocrystallites (10 – 30 nm) has been observed. The key role of the hexagonallike subsystem is demonstrated.

With increasing optically-poled UV laser (λ=337 nm) power of the output PISHG signal increases and achieves its maximum at the photoinducing power about 2.6 GW/cm^2 per pulse, temperature about 4.2 K and pump-probe delaying time about 20 ps for the parallel light polarisations between the pumping and probing beams. The performed molecular geometry optimization and norm-conserving PP self-consistent calculations unambiguously show that the photoinduced charge density non-centrosymmetry is originated from interfaces between the crystallites and surrounded amorphous-like background. Simultaneously significant role of the electron - phonon anharmonic contribution is proved. The maximal values of the obtained PISHG are equal about 1.02 pm/V and are comparable with the traditional nonlinear optical crystals. A good agreement between the experimental and theoretical data (energy gap, size-dimension effects, temperature-dependent pump-probe time kinetics and PISHG) indicates on a possibility of using the proposed approach for modeling of opto-electronics properties in such kinds of the

nanocrystallites. The existed discrepancies reflect a presence of the macrogradients and complications originated from phase-matching condition fulfilling.

ACKNOWLEDGEMENTS

The study was supported by the Polish State Committee for Scientific Research through grant No KBN – 8 - T11B 026 14.

REFERENCES

[1] W. Wang and A. Zunger, J.Phys.Chem., **98**, 2158 (1994).
[2] N.A.Hill and K.B. Whaley, Phys.Rev.Lett., **75**, 1130 (1995).
[3]A.Mews, A. V.Kadavanich, U.Banin, and A.P.Alivisatos, Phys.Rev., **B53**, 13242 (1996).
[4] C.R.Kagam, C.B.Murray, M.Nirmal, and M.G.Bawendi, Phys.Rev.Lett., **76**, 1517 (1995).
[5] D.J.Norris and M.G.Bawendi, Phys.Rev., **B53**, 16338 (1996).
[6] A.P.Alivisatos, Science, **271**, 933 (1996).
[7]C.B.Murray, D.J.Norris, and M.G.Bawendi, J.Am.Chem.Soc., **115**, 8706, (1993).
[8] A. J. Shields, M.Cardona, and K. Eberl, Phys. Rev. Letters, **72,** 412 (1994).
[9] H.Weller, Angew.Chem.Int.Ed.Engl., **105**,41 (1993).
[10] A.Haselbarth, A.Eychmuller, and H.Weller, Chem. Phys.Lett., **203**, 271 (1993).
[11] J.R.Heath, J.J.Shiang, and A.P.Alivisatos, J. Chem. Phys., **101**, 1607 (1994).
[12] V.Paillard, P.Puech, M.A.Laguna, and R.Carles, J. Appl. Phys., **86**, 1921 (1999).
[13] R.W.Schoenlen, D.M.Mittleman, J.J.Shiang, A.P.Alivisatos, and C.V.Shanh, Phys.Rev.Lett., **70**, 1014 (1993).
[14] Y. Li, M.Takata, and A.Nakamura, Phys.Rev., **B57**, 9193 (1998).
[15] V.L.Colvin, M.C.Schlamp, and A.P.Alivisatos, Nature, **370**, 354 (1994).
[16] F. Huisken, B.Kohn, and V. Paillard, Appl. Phys. Letters, **74**, 3776 (1999).
[17] W.L.Wilson, P.F.Szajowski, and L.E.Brus, Science, **262**, 1242 (1993).
[18] S.H.Tolbert, A.B.Herhold, S.B.Johnson, and A.P.Alivisatos, Phys.Rev.Lett., **73**, 3266 (1994).
[19] A.I.Ekimov, F.Kache, M.C.Shanneklein, D.Ricard, C.Flytzanis, J.A.Kudryavtsev, T.V.Yazeva, A.V.Rodina and A.L.Efros, J.Opt.Soc.Am., **B10**, 100 (1993).
[20] P.E.Lippens, Semicond. Sci.Technol., **6**, A157 (1991).
[21]. S.Ogut and J.R.Chelikowsky, Phys. Rev.Lett., **79**, 1770 (1997).
[22] C.Charpentier, A.Kassiba, J.Emery, and M.Cauchetier, J. Phys.Cond.Matter, **11**, 4887 (1999).
[23] J. M. Nunzi, J. M. Fiorini, C. Etile, and F. Kajzar, Pure Appl.Optics, **7**, 141 (1998).
[24] J.Wasylak, J.Kucharski, I.V.Kityk, and B.Sahraoui, J.Appl.Phys., **85**, 425 (1999).
[25] B.Sahraoui, I.V.Kityk, P.X.Phu, P.Huddhomme, and A.Gorgues, Phys. Rev., **B 59**, 9229 (1999).
[26] M.Malachowski, I.V.Kityk, and B.Sahraoui, Phys. Status Solidid, **207 B**, 405 (1998).